Published in final edited form as:
Proc SPIE. 2008 March 13; 6914: . doi:10.1117/12.772347.

A Deformable Model-based Minimal Path Segmentation Method for Kidney MR Images

Ke Li and
Case Western Reserve University and the University of Electronic Science and Technology of China

Baowei Fei*
Case Western Reserve University, Cleveland, OH

Abstract

We developed a new minimal path segmentation method for mouse kidney MR images. We used dynamic programming and a minimal path segmentation approach to detect the optimal path within a weighted graph between two end points. The energy function combines distance and gradient information to guide the marching curve and thus to evaluate the best path and to span a broken edge. An algorithm was developed to automatically place initial end points. Dynamic programming was used to automatically optimize and update end points during the searching procedure. Principle component analysis (PCA) was used to generate a deformable model, which serves as the prior knowledge for the selection of initial end points and for the evaluation of the best path. The method has been tested for kidney MR images acquired from 44 mice. To quantitatively assess the automatic segmentation method, we compared the results with manual segmentation. The mean and standard deviation of the overlap ratios are 95.19%±0.03%. The distance error between the automatic and manual segmentation is 0.82±0.41 pixel. The automatic minimal path segmentation method is fast, accurate, and robust and it can be applied not only for kidney images but also for other organs.

Keywords

Segmentation; minimal path; deformable model; dynamic programming; polycystic kidney disease; magnetic resonance imaging (MRI)

1. INTRODUCTION

Autosomal-dominant polycystic kidney disease (ADPKD) is a common genetic disorder, which lead to enlarged bilateral kidneys with multiple cysts. The severity of the renal functional impairment is associated with the size of the kidneys, where larger kidneys are found with poorer renal function [1]. Serial MRI studies can provide high-resolution anatomic structure of the kidneys and thus could be a useful tool for the assessment of various therapies [2]. We are investigating a transgenic mouse model for evaluating new therapeutic drugs. We are utilizing MR imaging for noninvasive monitoring and assessment. In this paper, we focus on automatic segmentation methods for mouse kidney MR images.

Automatic image segmentation methods use local image force at a specific point, but also on the properties of a contour's shape. Kass *et al.* proposed an active contour model [3], which

*Corresponding author: Department of Radiology and Imaging Sciences, Emory University, 1841 Clifton Road NE, Atlanta GA 30329. Phone: 404-712-5649, Baowei.Fei@emory.edu; Website: www.feilab.org.

is also termed as “snake” because of the feature of its evolution. The method provides an interactive tool for image segmentation and it has been investigated extensively among the model-based techniques. The minimization of the energy is controlled by two important forces, i.e. the internal energy that controls the smoothness of the contour, and the potential energy that attracts the contour toward the object boundary. However, this method has two limitations. First, it is sensitive to its initial position, especially for noised images. The second limitation is that it is not easy to deal with topological adaptation such as splitting or merging model parts, because a new parameterization must be constructed whenever the topology change occurs[17]. Geometric deformable models, proposed independently by Caselles *et al.* [6] and Malladi *et al.* [7], provide a solution to overcome the primary drawbacks of the active contour model. Geometric models are based on the curve evolution theory [8–11] and the level set method developed by Osher and Sethian [12, 13]. Osher and Sethian have also proven that a particular case of the classical energy snake model is equivalent to finding a geodesic or minimal distance path in a Riemannian space with a metric derived from the image content. This means that under a specific framework, boundary detection can be considered equivalent to finding a path of minimal weighted length via an active contour model based on geodesic or local minimal distance computation. The graph search method [14] and the fast march method [15] all search for the running cost in order to find the shortest path under this framework. The graph search methods, such as Dijkstra’s graph search method [14, 16] and Dynamic programming [19,20], use a grid with prescribed weights to find an optimal path. The fast march method is a computational technique that approximates the solution to nonlinear equations. The graph search methods solve minimal path problems much more directly than the fast marching method. However, they suffer from “metrication errors”. In other words, a rectangular grid with an equal unit weight will produce multiple paths between the two end points with the same cost [15].

To overcome this shortcoming, Cohen *et al.* proposed a global minimal path approach [17]. Their method detects the global minimum energy path between two end points. This approach does permit a better handling of the noise than the other active contour models, but it requires user intervention to mark some initial end points on the true boundary. Gerger *et al.* [14] and Yan *et al.* [18] took advantage of a priori knowledge as model to design a potential window as the search constraints for their dynamic programming active contour model. But two shortcomings of these methods also exist. It requires careful selection of initial position and it is sensitive to noise and broken edges.

We are developing dynamic programming and minimal path segmentation approach to detect the optimal path within a weighted graph between two end points. An energy function will combine distance and gradient information to guide the marching curve and thus to evaluate the best path and to span a broken edge. The segmentation algorithm could automate the placement of initial end points. Dynamic programming was used to automatically optimize and update end points during the searching procedure. Principle component analysis (PCA) was used to generate the deformable model, which was used as the prior knowledge for the selection of initial end points and for the evaluation of the best path.

The organization of the paper is as follows. In Section 2, we discuss the details of proposed method. In Section 3, the method is applied to segment kidney MR images from transgenic mice. The summary and conclusion are presented in Section 4.

2. METHODS

2.1 Energy Function

The traditional energy function of a snake is proposed by Kass *et al*. [5], which includes two important forces as follow:

$$E(C)=\alpha\int_{\Omega}|C'(\nu)|^2 d\nu+\beta\int_{\Omega}|C''(\nu)|^2 d\nu-\lambda\int_{\Omega}|\nabla I(C(\nu))|d\nu \quad (1)$$

Where α, β and λ denote real positive weighting constants; $\Omega \in [0,1]$ is the parameterization interval for the contour; ∇I represents the gradient of the image. Given the set of constants α, β and λ, the function can be solved to obtain the segmented contour C. Let $\beta = 0$ and ∇I be replaced by $g(|\nabla I|)^2$, the energy function becomes

$$E(C)=\alpha\int_{\Omega}|C'(\nu)|^2 d\nu+\lambda\int_{\Omega}g(|\nabla I(C(\nu))|)^2 d\nu \quad (2)$$

Where $g(|\nabla I|)^2$, is a potential function which is strictly decreasing, so that $g(r) \to 0$ as $r \to \infty$. A new function for minimizing (2) is equivalent to a problem of geodesic computation in a Riemannian space, proposed by Caselles *et al*. [5], as follows:

$$\min\int_{\Omega}g(|\nabla I(C(\nu))|)^2|C'(\nu)|d\nu \quad (3)$$

where the Euclidean length of the contour C is given by $L(C) = \int_{\Omega}|C'(\nu)|d\nu = \int_{\Omega}ds$. Therefore, the problem of image segmentation is transformed into a search for the global minimal path. This method is called as minimal path, which has lower computational complexity in high-order gradients and does not involve minimizing the corresponding Euler–Lagrange equation.

In this paper, we modify this function to improve the robustness because we found the distance map can lose important gradient information. We incorporated distance and gradient information into an energy function to guide the marching curve toward the best path and to span the broken edge. One term was added to the energy function, which represents the gradient information from the original image. Therefore, the energy function is

$$E(C)=\int_{\Omega}(\alpha E_{\mathrm{mod}\,el}+\beta E_{image}+\gamma E_{\mathrm{int}})d\nu \quad (4)$$

Where α, β and γ are real positive weighting constants which balance the forces, Ω denotes the current curve body, $E_{\mathrm{mod}\ el}$ can be calculated using Bayes' Rule and the maximum posteriori probability (MAP) function,

$$\Psi_{MAP}=\arg\min_{\Psi}\{\nu_1\int_{\Omega}|\Psi(C(s))|ds+\nu_2\int_{\Psi=0}G(x,y)dxdy+\frac{1}{2}\alpha^T\sum\nolimits_k^{-1}\alpha\} \quad (5)$$

where Ψ denotes the weighted graph that contains the estimated curve of the object, G(x, y) denotes the weighted graph of the image. The first term represents the degree of the current curve matching the estimated distance map, the second term represents the degree of the estimated distance map matching the former distance map, and the third term represents the probability of the estimated shape which is described later.

$$E_{image}=\lambda\int_C|C_s|ds-(1-\lambda)\int_C g(|\nabla I(C(\nu))|)^2 d\nu \quad (6)$$

where the first term denotes the degree of the curve C in the distance map, which is the Euclidean length of the curve C; the second item denotes the gradient of the original image, which is used to regulate the searching when the distance map is not enough for guiding the curve in case of noises and lack of a real edge. λ and (1-λ) denote the weights of the distance and gradient information.

$$E_{\text{int}}=\|\frac{\partial^2 C}{\partial S^2}\|, \text{in the discrete case}, E_{\text{int}}=\|P_{i-1}-2P_i+P_{i+1}\|, \text{is a smooth term.}$$

2.2 Kidney Model

The prior information is used to constrain the actual deformation of the contour or surface in order to extract the shape that is consistent with the training data or the prior model.

Several methods of incorporating prior shape information into boundary determination have been developed. Staib and Duncan [21] proposed a statistical deformable model using a Fourier representation. It is a direct parameterization method for representing curves and surfaces. Another approach was proposed by Pentland *et.al* and Nastar *et.al.* [22, 23], which is similar to the deformable Fourier model except that both the basic functions and the nominal values of their coefficients are derived from a template object shape. An extension of deformable models that incorporate local and global shape features is the deformable super quadric, proposed by Terzopoulos and Metaxas [24]. Active shape models (ASMs) are proposed by Cootes et al., which define a set of points at various features in the image [25, 26]. Ip and Shen incorporated prior shape information by using an affine transformation to align a shape template with the deformable model and to guide the model's deformation to produce a shape consistent with the template [27]. The deformable Fourier model, active shape model, and other extensions are all parametric deformable models. Fritsch *et al.* extracted the important shape features using information on the medial loci or cores of the shapes, which provides greater robustness to image disturbances such as noise and blurring than purely edge-based models. [28]

In this paper, the prior knowledge was incorporated into a deformable model for segmenting or localizing the anatomical structure. The deformable model for selecting initial end points and evaluating the best path is created in our algorithm. We computed and obtained a kidney shape model using the principal component analysis (PCA).

For training images, we first registered them using a custom-made program and then manually segmented the kidney on each image. We then performed distance transforming under a fixed size window. After computing the mean of the 1 training distance maps, we got a mean contour, $\overline{\mu}=\frac{1}{n}\sum\mu$.

Then, the variable μ is subtracted from each μ_i to create the mean-offset array μ_{offset}, which is placed as a column vector in an $N^d \times n$ dimensional matrix M. We computed and obtained a kidney shape model using the principal component analysis (PCA). After using singular value decomposition (SVD), the matrix is decomposed as $P = U\Sigma V^T$. Matrix U is the model with orthogonal column vectors that consist of the modes of shape variation and diagonal matrix Σ is composed of corresponding singular values. Given coefficient α and shape matrix U_k, we can estimate a new shape μ,

$$\mu = U_k \alpha + \overline{\mu} \quad (7)$$

Which is represented by k principal components in a k-dimensional vector of shape parameters α (where k < n). We assumed the shape parameter α was satisfied a Gaussian distribution as represented below:

$$P(\alpha) = \frac{1}{\sqrt{(2\pi)^k |\sum_k|}} \exp\left(-\frac{1}{2}\alpha^T \sum_k^{-1} \alpha\right) \quad (8)$$

2.3 Improved Dynamic Programming

In our method, the first step is transforming the image into a graph-based map. The graph-based search methods consider an image as a graph with a rectangular grid in which each pixel is a node. Boundary definition via dynamic programming can be formulated as a graph searching problem where the goal is to find the optimal path between a set of start nodes and a set of end nodes. The optimal path is defined as the minimum cumulative cost path, where the cumulative cost of a path is the sum of the local costs of the pixels on the path.

To overcome the difficult of searching the initial direction in dynamic programming, we define a universal direction window, any direction searching window map must be transformed into this universal direction searching window. In the step of searching the minimal path by dynamic programming, each point have three children points, and each children point also has each three children points in the next step, so the universal searching window looks like a triangle area. We defined the center point of the start line in this window as the start stage of dynamic programming, and defined the each point of the end line as the end stage. So, if there are n points in the end line, there are n optional paths generated in our one path searching. We can obtain several optional results for evaluation. The best path is then selected using former energy function.

3. EXPERIMENTS AND RESULTS

We acquired kidney MR images from 44 mice using a Siemens Sonata 1.5 T scanner. A three-dimensional (3D) True FISP pulse sequence (TR/TE= 10.4/5.2ms) with a slice thickness of 500 μm was used to generate high-resolution coronal images (matrix: 256 × 192, FOV: 67 × 50-mm).

Incorporation of prior knowledge requires a training step that involves manual interaction to accumulate information on the variability of the object shape being delineated. This information is then used to constrain the actual deformation of the contour or surface to extract shapes consistent with the training data. We randomly selected 20 dataset for model training, and used the other 24 datasets to test the segmentation method.

For the training images, we first registered and manually segmented the 20 kidney dataset on each image. We then performed distance transformation under a defined window size. After computing the mean of the training distance maps, we got a mean contour. Then, the variable μ is subtracted from each to create the mean-offset array, which is placed as a column vector in an N dimensional matrix M. After using the formulas (4) and (5), we obtained the mean shape contour and singular value and orthogonal.

After the generation of our kidney model, we segmented the other 24 mice kidney dataset. Before segmentation, the image was preprocessed by Canny edge detection [29] and distance transform [30]. Figure 1 shows the procedure of creating and updating serial end

points for minimal path searching. We set the goal object in the center of our rectangular searching window. Then, we selected the window center as the central point to create radius rays with an interval of a fixed angle (22.5 degrees in our case). If the weight value on the rays is zero in the distance map, it is marked as an end point, no matter what it is on the fake or real edge because of noise or edge discontinuity. If not, we selected the intersection point between the rays and mean segmented contour of the model as the marked end point. Thus, a sequence of marked end points was generated.

At the beginning of searching the minimal path using dynamic programming, we selected every two interval adjacent-end points and several neighbor points of the subsequent end points as the start and end stages for dynamic programming. After the procedure of dynamic programming between start and end stages, we finished the path searching one time. Because the start stage has one end point and the end stage has several end points, several paths are generated and a best path with minimal energy will be selected. We used the function (4) to evaluate and select the minimal energy path. We selected the middle point of this minimal path as the next starting end point, rather than the next point of the original alignment. From this new starting point to its interval point, a new searching procedure was started again. Thus, the marked end points were continuously updated and optimized towards the direction of the real edge. We can set the number of iterations or can control the error rate between two iterations as the stopping condition. After several iterations, a satisfied segmented contour could be obtained. The result contour is on or approaching the real edge because of the influence of maximum probability of the model. We can get the satisfied result, even if a part of real edge was lost on the image.

Figure 2 demonstrates the steps for the minimal path segmentation, which include Canny edge detection, distance transform, gradient map, and the minimal path segmentation.

The segmentation was evaluated by the overlap ratio between automatic and manual segmentation and by mean distance errors between the two segmentations. The overlap ratio is calculated as the ratio of superposition between our automatic segmentation results and the manual segmentation results. The distance error is the distance between a point on one segmented contour and its closest point on the other segmented contour. The mean distance error is the mean of all points on the contour. For MR images from 24 mice, the overlap ratio is 0.93%±0.05% between automatic and manual segmentation and the distance error is 0.85±0.41 pixel. The method is accurate and robust for mouse kidney MR images. For “bad” images with many noises and the broken edges, our method also achieved satisfied results. Figure 3 shows four different images and the segmentation results. The method works well for both “good” and “bad” images as well as for images with discontinuous edges.

4. DISCUSSIONS AND CONCLUSIONS

We developed a new, automatic, minimal path segmentation method for mouse kidney MR images. To improve the robustness, we incorporated distance and gradient information into the energy function in order to guide the marching curve toward the best path. We also incorporated a prior knowledge model into the segmentation in order to span broken edges. Dynamic programming was used to automatically update the end points. Preliminary results from 44 mouse demonstrated that this method is fast, accurate, and robust for kidney MR images. The method was implemented in two-dimensional images and we are extending it to three-dimensional image volumes. We believe that this method can be applied not only for kidney images but also for other organs.

Acknowledgments

The algorithm developed in this research was partially supported by the NIH grant R21CA120536 (PI: Fei), the Presidential Research Initiate Award from Case Western Reserve University (PI: Fei) and the Case Comprehensive Cancer Center Pilot Project Award (PI: Fei). The Case Center for Imaging Research is supported by the NIH/NCI R24 grant (CA110943).

References

1. Gabow PA, Johnson AM, Kaehny WD, et al. Factors affecting the progression of renal disease in autosomal-dominant polycystic kidney disease. Kidney Int. 1992; 41:1311–1319. [PubMed: 1614046]
2. Fei, B.; Flask, C.; Wang, Hs, et al. Image Segmentation, Registration and Visualization of Serial MR Images for Therapeutic Assessment of Polycystic Kidney Disease in Transgenic Mice. Proceedings of the 27th Annual Conference of IEEE Engineering in Medicine and Biology Society (EMBS); 2005. p. 467-469.
3. Kass M, Witkin A, Terzopoulos D. Snake: Active contour models. Int J Comput Vis. 1987; 1(4): 321–331.
4. Durikovic R, Kaneda K, Yamashita H. Dynamic contour: a texture approach and contour operations. The Visual Computer. 1995; 11:277–289.
5. McInerney, T.; Terzopoulos, D. Topologically adaptable snakes. Proc. 5th Int'l Conf. Comp. Vis; 1995. p. 840-845.
6. Caselles V, Catte F, Coll T, Dibos F. A geometric model for active contours. Numerische Mathematik. 1993; 66:1–31.
7. Malladi R, Sethian JA, Vemuri BC. Shape modeling with front propagation: a level set approach. IEEE Trans Patt Anal Mach Intell. 1995; 17(2):158–175.
8. Sapiro G, Tannenbaum A. Affine invariant scale-space. Int'l J Comp Vis. 1993; 11(1):25–44.
9. Kimia BB, Tannenbaum AR, Zucker SW. Shapes, shocks, and deformations I: the components of two-dimensional shape and the reaction-diffusion space. Int'l J Comp Vis. 1995; 15:189–224.
10. Kimmel R, Amir A, Bruckstein AM. Finding shortest paths on surfaces using level sets propagation. IEEE Trans Patt Anal Mach Intell. 1995; 17(6):635–640.
11. Alvarez L, Guichard F, Lions PL, Morel JM. Axioms and fundamental equations of image processing. Archive for Rational Mechanics and Analysis. 1993; 123(3):199–257.
12. Osher S, Sethian JA. Fronts propagating with curvature-dependent speed: algorithms based on Hamilton-Jacobi formulations. J Computational Physics. 1988; 79:12–49.
13. Sethian, JA. Level Set Methods and Fast Marching Methods: Evolving Interfaces inComputational Geometry. 2. Cambridge University Press; Cambridge, UK: 1999.
14. Mortensen EN, Barrett WA. Interactive segmentation with intelligent scissors. Graph Mod Image Process. 1998; 60(5):349–384.
15. Sethian JA. Fast marching methods. SIAM Rev. 1999; 41(2):199–235.
16. Dijkstra EW. A note on two problems in connection with graphs. Numer Math. 1959; 1:269–271.
17. Cohen LD, Kimmel R. Global minimum for active contour models: A minimal path approach. Int J Comput Vis. 1997; 24(1):57–78.
18. Yan PK, Kassim AA. Medical Image Segmentation Using Minimal Path Deformable Models With Implicit Shape Priors. IEEE Trans Info Tech in Bio. 2006; 10(4):677–684.
19. Amini AA, Weymouth TE, et al. Using Dynamic Programming for Solving Variational Problems in Vision. IEEE Trans Pattern Analysis and Machine Intelligence. 1999; 12(9):855–867.
20. Udupa JK, Saha PK, Lotufo RA. Boundary detection via dynamic programming. in Proc SPIE Med Imaging. 1992; 1808:33–39.
21. Staib LH, Duncan JS. Boundary finding with parametrically deformable models. IEEE Trans Patt Anal Mach Intell. 1992; 14(11):1061–1075.
22. Pentland A, Horowitz B. Recovery of nonrigid motion and structure. IEEE Trans Patt Anal Mach Intell. 1991; 13:730–742.

23. Nastar C, Ayache N. Frequency-based nonrigid motion analysis: application to four dimensional medical images. IEEE Trans Patt Anal Mach Intell. 1996; 18:1067–1079.

24. Terzopoulos D, Metaxas D. Dynamic 3D models with local and global deformations: deformable superquadrics. IEEE Trans Patt Anal Mach Intell. 1991; 13:703–714.

25. Cootes TF, Hill A, Taylor CJ, Haslam J. Use of active shape models for locating structures in medical images. Imag Vis Computing J. 1994; 12(6):355–366.

26. Cootes TF, Taylor CJ, Cooper DH, Graham J. Active shape models – their training and application. Comp Vis Imag Under. 1995; 61(1):38–59.

27. Ip HHS, Shen D. An affine-invariant active contour model (AI-snake) for model-based segmentation. Imag Vis Computing J. 1998; 16:135–146.

28. Fritsch D, Pizer S, Yu L, Johnson V, Chaney E. Segmentation of medical image objects using deformable shape loci. in Proc Information Processing in Medical Imaging (IPMI'97). 1997:127–140.

29. Canny J. A computational approach to edge detection. IEEE Trans Pattern Anal Mach Intell. 1986; 8(6):679–698. [PubMed: 21869365]

30. Breu H, Gil J, Kirkpatrick D, Werman M. Linear time euclidean distance transform algorithms. IEEE Trans Pattern Anal Mach Intell. 1995; 17(5):529–533.

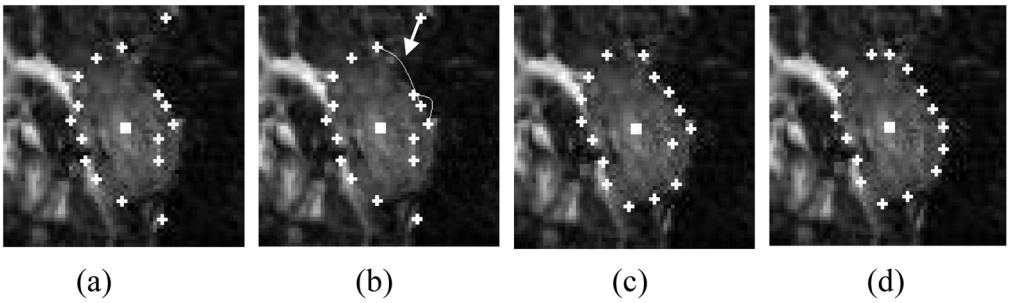

Fig. 1.

Procedure for selecting and updating end points. (a) Initial end points. Radial rays were generated from the window center of the distance map. If the weighting value of a point along the ray is zero, it is marked as an end point. If not, select the intersection point between the ray and the mean contour of the model as the marked end point. (b) Update end points. If there is a broken edge and the end point is far away from the real edge, the algorithm will use the model. The end point will be corrected towards the real edge (Arrow) after iterations. (c)–(d) End Points after one and two iterations, respectively.

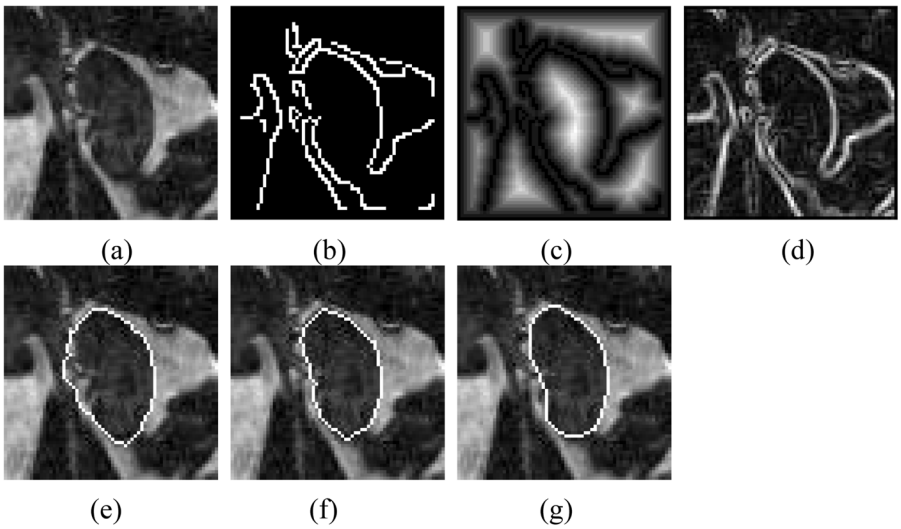

Fig. 2.

Steps for the minimal path segmentation. (a) Original image. (b) Edge map generated from the original image using Canny edge detection. (c) Distance map generated from the edge map using Euclidean distance transform. (d) Gradient map generated from the original image. (e) and (f) Results from the minimal path segmentation without using the gradient map (λ=1) and with the gradient and distance information (λ=0.8), respectively. (g) Manual segmentation result.

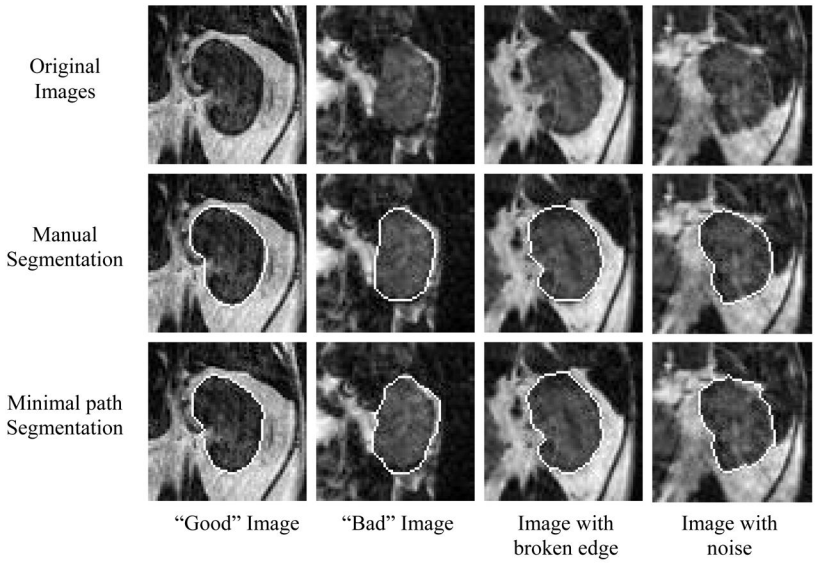

Fig. 3.

Automatic segmentation results for images with different quality. Image (a) is a typical mouse kidney MR image. The boundaries of the kidney on the images (b), (c) and (d) are not continuous. The automatic segmentation method works well for all the images.